Title
Electric current control of creation and annihilation of sub-100 nm magnetic bubbles examined by full-field transmission soft X-ray microscopy

Journal
Current Applied Physics, 18(11)

ISSN
1567-1739

Authors
Je, Soong-Geun
Jung, Min-Seung
Im, Mi-Young
et al.

Publication Date
2018-11-01

DOI
10.1016/j.cap.2018.06.004

Peer reviewed

Electric Current Control of Creation and Annihilation of Weakly Chiral Magnetic Skyrmions Examined by Full-Field Transmission Soft X-ray Microscopy

Soong-Geun Je,[1,2] Min-Seung Jung,[2] Mi-Young Im,[1,2,3,*] and Jung-Il Hong[2,*]

[1]Center for X-ray Optics, Lawrence Berkeley National Laboratory, Berkeley, California 94720, USA

[2]Department of Emerging Materials Science, Daegu Gyeongbuk Institute of Science & Technology, Daegu 42988, Korea

[3]School of Materials Science and Engineering, Ulsan National Institute of Science and Technology (UNIST), Ulsan 44919, Korea

[*]Emails: jihong@dgist.ac.kr, mim@lbl.gov

The effect of electric current pulses on a magnetic skyrmion state in a symmetric Pt/Co multilayer was directly observed using a full-field transmission soft X-ray microscope (MTXM). Field-induced evolution of the magnetic stripe domains into isolated weakly chiral skrymions with their sizes down to 100 nm was imaged under varying external magnetic fields. Electric current pulses were then applied to the created magnetic skyrmions, and it was observed that the skyrmions could be either created or annihilated by the current pulse depending on the strength of applied magnetic field. The results suggest that the Joule heating plays a critical role in the formation and/or elimination of the skyrmions, hence an optimized scheme with the combination of magnetic field and electric current is necessary to utilize skyrmions in the practical devices.

In response to the ever-growing demands for data storage, utilization of magnetic skyrmions in the future information technology has risen as one of the possible alternatives with the prospect to achieve high density memory devices operated with low power consumption due to their topologically protected nature as well as their small sizes [1]. Magnetic skyrmions were initially observed in bulk materials with non- centrosymmetric crystal lattices [2-3], but skyrmions in ultrathin materials where magnetic layers are interfaced by heavy metal layers with strong spin-orbit couplings, are attracting a growing attentions of current research communities. In an ultrathin magnetic film, the interfacial Dzyaloshinskii-Moriya interaction (DMI) induces a preferred Neel domain wall direction, resulting in skyrmions of fixed chirality [4,5]. Then the spin-orbit torque (SOT) due to the charge current flowing through the adjacent heavy metal layer and/or the interface can manipulate the chiral skyrmions in a controlled way [6], making the skyrmions in the thin film materials particularly appealing.

Both DMI and SOT were found to have significant impacts on the skyrmion behaviors, and extensive researches on them are in progress worldwide. The SOT-induced skyrmion motion [7,8], skyrmion Hall effect [9] and SOT-induced generation of skyrmions [10] have experimentally been demonstrated. Recently, more practical conditions in a realistic situation, such as the Joule heating effect [11], which inevitably exists when generating SOT, and the disorder effect [12], which is generally present in sputtered magnetic films, have begun to be taken into consideration. In this regard, the direct observation of small skyrmions on a length scale of tens of nanometer and their reactions to injected current pulses in a system with weak SOT and DMI can offer an insight into what is actually happening in the skyrmion-based devices.

In the present work, we show the electric current effects on skyrmions with the size down to 100 nm in a symmetric Pt/Co multilayer stack in which SOT is suppressed. Using a full-field transmission soft x-ray microscope, magnetic structures along the magnetic hysteresis curve measured by vibrating sample magnetometer (VSM) were imaged. Under certain fields, a weak-chiral skyrmion phase was observed. The effect of current pulses on the skyrmions was investigated by injecting current to the magnetic field-stabilized skyrmions. It is found that the electric current with little SOT contribution either increases or decreases the density of the skyrmions depending on the strength of the applied field even with the same current pulses. We attribute this observed phenomenon to Joule heating and changes in the energy barriers for the creation and annihilation of the skyrmions depending on the strength of the

applied magnetic field.

For this study, 20-μm-wide [Pt (3 nm)/Co (1 nm)]$_{15}$/Pt (3 nm) multilayer track was fabricated using photolithography and lift-off processes. Multilayer stack was grown by dc magnetron sputtering. The track structure allows electric currents to flow in a well-defined direction. As the magnetic layers are sandwiched by the Pt layers of the same thickness, when currents are flowing through the track, the SOT effects, mainly exerted by the spin currents coming from the neighboring top and bottom Pt layers via the spin Hall effect, are anticipated to be cancelled [13], making this system appropriate for the study of the electric current effect with minimal SOT. The fifteen repetition is intended to enhance the magnetic contrast in the X-ray magnetic circular dichroism (XMCD) and also to increase the demagnetizing field which is crucial for the stabilization of the bubble structure. The stack is deposited on a Si_3N_4 membrane with the thickness of 100 nm for the X-ray transmission. The magnetic images were acquired using a full-field magnetic transmission soft x-ray microscope, XM-1, at the beamline 6.1.2 at the Advanced Light Source [14].

Figure 1 shows the magnetization curve obtained using VSM and the MTXM images of the magnetic domains along the hysteresis curve as indicated by the arrows. The magnetization curve was measured with the identical film structure grown on Si substrate. At zero field, as shown in the image at the center of Fig. 1, a demagnetized labyrinthine domain (~150 nm wide) state is dominantly observed, and this is consistent with the nearly diminished magnetization at the corresponding field in the magnetization curve. As the magnetic field increases along the right branch of the hysteresis loop, the magnetic domains initially shrink in the lateral direction (width) rather than in the longitudinal direction (length), implying the strong pinnings at the domain ends. By further increasing the magnetic field, lateral compression finally results in the fission of the stripe domains into isolated skyrmions with the size of around 100 nm (top right image in Fig. 1). It is worth noting that a finite DMI was reported even in the symmetric Pt/Co (0.3 nm)/Pt stacks [13,15]. However, with nominally 1 nm thickness of the individual Co layers in the present stack, the interfacial DMI might be insufficient [16] to stabilize the chiral Néel domain walls. In this respect, we refer to the observed magnetic domains as weakly chiral skyrmions. Further investigation might be required to demonstrate the chiral nature of the present spin texture using other imaging techniques [5, 17].

After the magnetic state fully saturated by further increasing the field up to 2.5 kOe, the external magnetic field was then gradually reduced. At a magnetic field of 680 Oe (top left of Fig. 1), abrupt nucleation of skyrmions were observed accompanied with the corresponding drop in the magnetization curve. The spontaneous nucleation of skyrmions can be understood in association with the strong demagnetizing field at the nucleation sites where the effective anisotropy energy landscape may exhibit local minima. As the applied magnetic field reduces to zero, some of the nucleated bubbles expanded and became worm-like domains while keeping their isolated topology.

Next, the impact of electric currents on weakly chiral skyrmions was investigated. In order to prepare the initial skyrmion state, the magnetic field was reduced to zero from 2.5 kOe and the field was increased to the values indicated in Fig. 2. For the prepared skyrmion states, electric current pulse with the duration time of 1ms and the current density of 7.6×10^{9} A/m^{2} was injected thorough the track and the MTXM images were taken after each current pulse injection. It is notable that the identical current pulse leads to distinctly different results under the two different magnetic fields. At the low magnetic field of 210 Oe [Fig. 2(a-c)], additional skyrmions are nucleated by the first current pulse and the subsequent current pulse does not make any notable changes in the number of bubbles. On the other hand, at the high magnetic field of 680 Oe [Fig. 2(d-f)], the initial skyrmions are annihilated by the first pulse, resulting in the saturated magnetic state. The saturated magnetic state is maintained under the subsequent pulse injection.

Since the application of identical current pules have been employed, the effects of Joule heating and SOT are expected to be the same for both events of the creation and annihilation of skyrmions. However, as the top and bottom of Co layers are in contact with Pt layers of identical thickness, net SOT might be cancelled out in the system and thereby, the role of SOT in the creation and annihilation processes would be insignificantly small.

In this circumstance, current-induced creation and annihilation of the skyrmions can be understood by the isolated bubble model [18,19] combined with Joule heating [11]. In the analytic bubble model, the size of the stabilized bubble and the energy barrier for its creation are determined by the competitions among the dipolar energy, domain wall energy, and Zeeman energy. The free energy of the isolated bubble as a function of its radius is known to have a typical shape as schematically shown in Fig. 3. The energy curve has a bump at a

small radius and there exist a local energy minimum at a certain radius, which corresponds to the radius of the stabilized bubble. When the applied field is weak, the local minimum of bubble state is a global minimum in the free energy (red curve in Fig. 3). Here, the creation of the bubble can be achieved by overcoming the bump in the free energy from zero radius corresponding to a fully saturated state. In this case, the Joule heating produced by the injected current pulse provides sufficient energy for the saturated state to reach the bubble state (red dashed line) by overcoming the energy barrier (red dashed line). It is observed that the pre-existing and newly created bubbles remain stable after subsequent current pulses [Fig. 2(b, c)], which confirms that the bubble state is the global energy minimum.

Since the external field is intended to shrink the domains, it is directed opposite to the magnetization of the center of the bubble (in Fig. 3). Thus, the Zeeman energy tends to increase the overall energy of the bubble. In the case of the strong magnetic field application, the local energy minimum of the bubble then becomes metastable due to the increased Zeeman energy contributions (blue curve in Fig.3) and the saturated state becomes the lowest energy state. Current-induced Joule heating assists the bubble to escape the metastable state, resulting in the annihilation (blue dashed line). Since the initial skyrmions have followed the local energy minimum path (equilibrium process), the initial skyrmions under the strong field [Fig. 2(d)] remain metastable until the system is perturbed by Joule heating.

The observation of the current-induced creation and annihilation of weakly chiral skyrmions in the SOT suppressed system highlights the role of Joule heating in the operation of skyrmion-based devices. In this regard, it can be concluded that the driving current needs to be lower than those for the creation and annihilation of skyrmions since the electric current inevitably accompanies Joule heating. High driving current with the purpose to increase SOT effect and thus to induce fast skyrmion motions may lead to unintended nucleation and/or annihilation of skyrmions. In order to avoid this, the SOT needs to be significantly enhanced so that Joule heating can be minimized. This can be accomplished by sandwiching two heavy metal layers of opposite spin Hall angles with a magnetic layer [20]. Alternatively, deposition of an oxide layer on top of the device might be useful as the oxide layer can serve as a heat sink without the shunting current. One can consider exploiting the Joule heating for a skyrmion writing scheme [11], but this inevitably demands a localized heating scheme.

In summary, we have revealed that stripe domains can transform to skyrmions with the sizes

smaller than 100 nm by applying an external magnetic fields and current pulses simultaneously. Direct observation of magnetic configurations using transmission soft X-ray microscopy showed that the pulses can trigger both creations and annihilations of skyrmions in a symmetric Pt/Co multilayer system with minimal DMI effect. It is emphasized that an identical current pulse can either create or annihilate skyrmions depending on the strength of the simultaneously applied external magnetic field. These creation and annihilation processes were understood in the framework of the isolated bubble energy model and the Joule heating. In particular, the creation of weakly chiral skyrmions as demonstrated in the present work induced by Joule heating without SOT may also have an implication on recent researches in the field of current-driven skyrmion motion where the Joule heating have mostly been ignored so far.

Acknowledgments

Authors acknowledge the financial supports from the Korean National Research Foundation (NRF) under the grant numbers of 2012K1A4A3053565, 2016K1A3A7A09005336, 2016K1A3A7A09005241, 2015M3D1A1070465, and 2016M3D1A1027831. DGIST R&D program (17-BT-02) is also acknowledged. Works at the ALS were supported by U.S. Department of Energy (DE-AC02-05CH11231).

References

[1] J. Sampaio, V. Cros, S. Rohart, A. Thiaville, and A. Fert, Nat. Nanotechnol. 8, 839-844 (2013).

[2] S. Mühlbauer, B. Binz, F. Jonietz, C. Pfleiderer, A. Rosch, A. Neubauer, R. Georgii, and P. Böni, Science 323, 915-919 (2009).

[3] X. Z. Yu, Y. Onose, N. Kanazawa, J. H. Park, J. H. Han, Y. Matsui, N. Nagaosa, and Y. Tokura, Nature 465, 901–904 (2010).

[4] C. Moreau-Luchaire, C. Moutafis, N. Reyren, J. Sampaio, C. A. F. Vaz, N. Van Horne, K. Bouzehouane, K. Garcia, C. Deranlot, P. Warnicke, C. Moreau-Luchaire, C. Moutafis, N. Reyren, J. Sampaio, C. A. F. Vaz, N. Van Horne, K. Bouzehouane, K. Garcia, C. Deranlot, P. Warnicke, P. Wohlhüter, J.-M. George, M. Weigand, J. Raabe, V. Cros, and A. Fert, Nat. Nanotechnol. 11, 444–448 (2016).

[5] Olivier Boulle, Jan Vogel, Hongxin Yang, Stefania Pizzini, Dayane de Souza Chaves, Andrea Locatelli, Tevfik Onur Menteş, Alessandro Sala, Liliana D. Buda-Prejbeanu, Olivier Klein, Mohamed Belmeguenai, Yves Roussigné, Andrey Stashkevich, Salim Mourad Chérif, Lucia Aballe, Michael Foerster, Mairbek Chshiev, Stéphane Auffret, Ioan Mihai Miron, and Gilles Gaudin, Nat. Nanotechnol. 11, 449–454 (2016).

[6] A. Fert, V. Cros, and J. Sampaio, Nat. Nanotechnol. 8, 152–156 (2013).

[7] Seonghoon Woo, Kyung Mee Song, Hee-Sung Han, Min-Seung Jung, Mi-Young Im, Ki-Suk Lee, Kun Soo Song, Peter Fischer, Jung-Il Hong, Jun Woo Choi, Byoung-Chul Min, Hyun Cheol Koo, and Joonhyeon Chang, Nat. Comm. 8, 15573 (2017).

[8] Wanjun Jiang, Pramey Upadhyaya, Wei Zhang, Guoqiang Yu, M. Benjamin Jungfleisch, Frank Y. Fradin, John E. Pearson, Yaroslav Tserkovnyak, Kang L. Wang, Olle Heinonen, Suzanne G. E. te Velthuis, and Axel Hoffmann, Science 349, 283–286 (2015).

[9] Kai Litzius, Ivan Lemesh, Benjamin Krüger, Pedram Bassirian, Lucas Caretta, Kornel Richter, Felix Büttner, Koji Sato, Oleg A. Tretiakov, Johannes Förster, Robert M. Reeve, Markus Weigand, Iuliia Bykova, Hermann Stoll, Gisela Schütz, Geoffrey S. D. Beach, and Mathias Kläui, Nat. Phys. 13, 170–175 (2017).

[10] Felix Büttner, Ivan Lemesh, Michael Schneider, Bastian Pfau, Christian M. Günther, Piet Hessing, Jan Geilhufe, Lucas Caretta, Dieter Engel, Benjamin Krüger, Jens Viefhaus, Stefan Eisebitt, and Geoffrey S. D. Beach, Nat. Nanotechnol. 12, 1040-1044 (2107).

[11] William Legrand, Davide Maccariello, Nicolas Reyren, Karin Garcia, Christoforos Moutafis, Constance Moreau-Luchaire, Sophie Collin, Karim Bouzehouane, Vincent Cros, and Albert Fert, Nano Lett. 17, 2703–2712 (2017).

[12] R. Juge, S.-G. Je, D. de Souza Chaves, S. Pizzini, L. D. Buda-Prejbeanu, L. Aballe, M. Foerster, A. Locatelli, T. O. Menteş, A. Sala, F. Maccherozzi, S. S. Dhesi, S. Auffret, G. Gaudin, J. Vogel, and O. Boulle, J. Magn. Magn. Mater. 455, 3-8 (2018).

[13] Soong-Geun Je, Sang-Cheol Yoo, Joo-Sung Kim, Yong-Keun Park, Min-Ho Park, Joon Moon, Byoung-Chul Min, and Sug-Bong Choe, Phys. Rev. Lett. 118, 167205 (2017).

[14] P. Fischer, D.-H. Kim, W. Chao, J. A. Liddle, E. H. Anderson, and D. T. Attwood, Mater. Today 9, 26–33 (2006).

[15] Soong-Geun Je, Duck-Ho Kim, Sang-Cheol Yoo, Byoung-Chul Min, Kyung-Jin Lee, and Sug-Bong Choe, Phys. Rev. B 88, 214401 (2013).

[16] Jaehun Cho, Nam-Hui Kim, Sukmock Lee, June-Seo Kim, Reinoud Lavrijsen, Aurelie Solignac, Yuxiang Yin, Dong-Soo Han, Niels J. J. van Hoof, Henk J. M. Swagten, Bert Koopmans, and Chun-Yeol You. Nat. Commun. 6, 7635 (2015).

[17] Shawn D. Pollard, Joseph A. Garlow, Jiawei Yu, Zhen Wang, Yimei Zhu, and Hyunsoo Yang, Nat. Commun. 8, 14761 (2017).

[18] N. Saratz, U. Ramsperger, A. Vindigni, and D. Pescia, Phys. Rev. B 82. 184416 (2010).

[19] M. Schott, A. Bernand-Mantel, L. Ranno, S. Pizzini, J. Vogel, H. Béa, C. Baraduc, S. Auffret, G. Gaudin, and D. Givord, Nano Lett. 17, 3006 (2017).

[20] Seonghoon Woo, Maxwell Mann, Aik Jun Tan, Lucas Caretta, and Geoffrey S. D. Beach, Appl. Phys. Lett. 105, 212404 (2014).

Figure 1

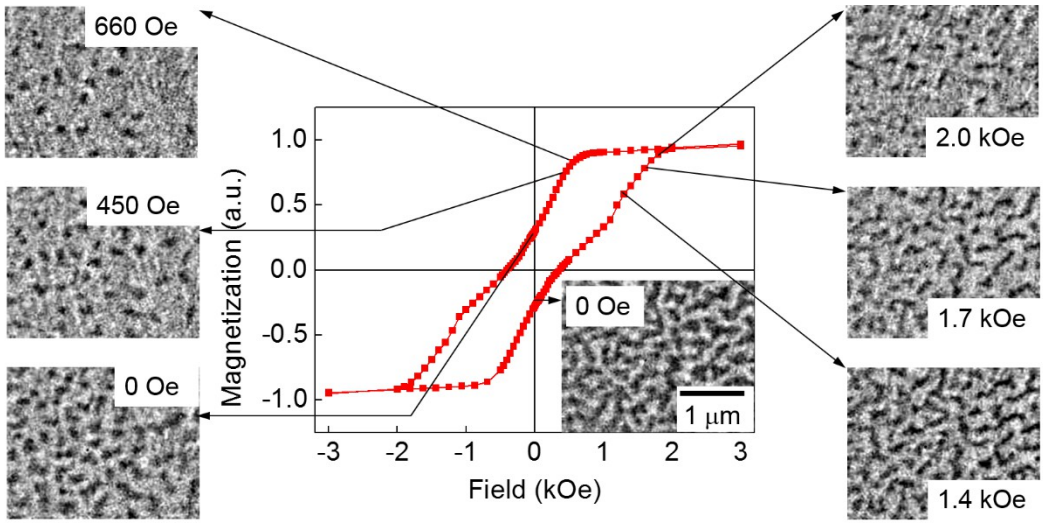

Figure 1. Magnetization curve and MTXM images acquired at increasing (on the right) and decreasing (on the left) fields. The images with decreasing fields are taken after positive field saturation. Black and white contrast correspond to the down magnetization and up magnetization, respectively.

Figure 2

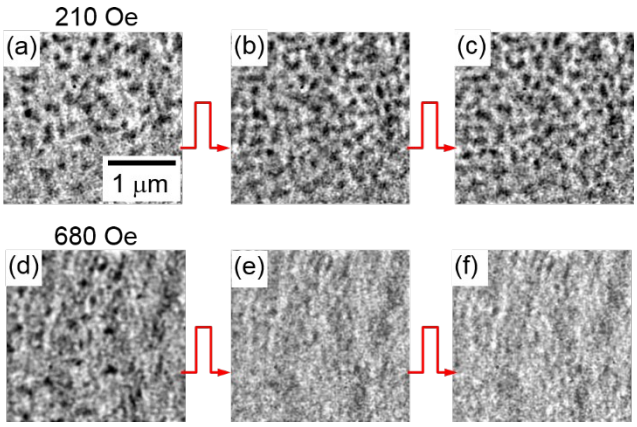

Figure 2. MTXM images taken after injecting the electric current pulse at the applied field of 210 Oe (a-c) and 680 Oe (d-f).

Figure 3

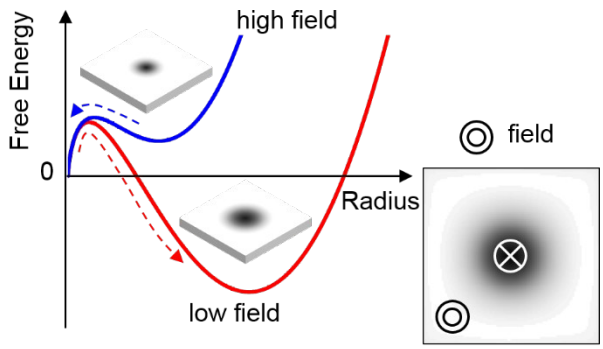

Figure 3. Schematic diagram of the bubble free energy with respect to the bubble radius under a low magnetic field (red solid line) and a high magnetic field (blue solid line). Dashed lines indicate the energetically favored paths when they are perturbed by Joule heating.